

COULD JUPITER OR SATURN HAVE EJECTED A FIFTH GIANT PLANET?

RYAN CLOUTIER^{1,2}, DANIEL TAMAYO^{2,3}, AND DIANA VALENCIA^{2,1}

Draft version August 20, 2018

ABSTRACT

Models of the dynamical evolution of the early solar system following the dispersal of the gaseous protoplanetary disk have been widely successful in reconstructing the current orbital configuration of the giant planets. Statistically, some of the most successful dynamical evolution simulations have initially included a hypothetical fifth giant planet, of ice giant mass, which gets ejected by a gas giant during the early solar system’s proposed instability phase. We investigate the likelihood of an ice giant ejection event by either Jupiter or Saturn through constraints imposed by the current orbits of their wide-separation regular satellites Callisto and Iapetus respectively. We show that planetary encounters that are sufficient to eject an ice giant, often provide excessive perturbations to the orbits of Callisto and Iapetus making it difficult to reconcile a planet ejection event with the current orbit of either satellite. Quantitatively, we compute the likelihood of reconciling a regular Jovian satellite orbit with the current orbit of Callisto following an ice giant ejection by Jupiter of $\sim 42\%$ and conclude that such a large likelihood supports the hypothesis of a fifth giant planet’s existence. A similar calculation for Iapetus reveals that it is much more difficult for Saturn to have ejected an ice giant and reconcile a Kronian satellite orbit with that of Iapetus (likelihood $\sim 1\%$), although uncertainties regarding the formation of Iapetus, on its unusual orbit, complicates the interpretation of this result.

Subject headings: methods: numerical — planets and satellites: dynamical evolution and stability

1. INTRODUCTION

Various solar system formation models argue that the giant planets underwent planetesimal driven migration (e.g. Fernandez & Ip 1984; Malhotra 1995; Hahn & Malhotra 1999; Tsiganis et al. 2005) at early times ($\lesssim 1$ Gyr) following a dynamical instability. The *Nice model*, originally presented by Gomes et al. (2005), Morbidelli et al. (2005), and Tsiganis et al. (2005), with subsequent variants under the same name, has been the most successful in reproducing the settling of the four giant planets into their present orbital configuration (Tsiganis et al. 2005; Morbidelli et al. 2007; Levison et al. 2011), the Late Heavy Bombardment at ~ 700 Myr (Gomes et al. 2005), the capture of Jupiter’s Trojan asteroids (Morbidelli et al. 2005), the capture of gas giant irregular satellites (Nesvorný et al. 2007), as well as the structure of the Kuiper belt (Levison et al. 2008) and how its dynamical evolution led to the contamination of the outer asteroid belt by primitive trans-Neptunian objects (Levison et al. 2009).

The precise nature of giant planet migration in the early solar system remains uncertain due to our lack of knowledge regarding each body’s initial conditions following their formation out of the solar nebula and the chaotic nature of the migration process. However, Morbidelli et al. (2009) argued that smooth divergent migration of the gas giants is unable to sufficiently excite their orbital eccentricities and inclinations to their observed values. Additionally, Brasser et al. (2009) showed

that such migration from an initial resonant configuration following the dispersal of the gaseous disk leads to excessive orbital eccentricities in the previously formed terrestrial bodies via sweeping secular resonances. A proposed solution, known as the *jumping-Jupiter scenario* (Brasser et al. 2009), invokes close encounters between the gas giants and an ice giant (IG) resulting in the step-wise migration of Jupiter and Saturn from their initial mean-motion resonance. This can sufficiently excite giant planet eccentricities and inclinations whilst jumping over the problematic secular frequencies of the terrestrial planets. In addition, the *jumping-Jupiter scenario* does not disrupt the asteroid belt’s observed morphology (Morbidelli et al. 2010).

A statistical study by Nesvorný (2011) of the dynamical evolution of the solar system during such a phase of frequent planetary encounters showed that the likelihood of reconstructing the current orbital configuration of the four giant planets is increased when a fifth giant planet of approximately Uranian mass is included in the early solar system. The instability, which gives rise to multiple planetary encounters, results in the ejection of the hypothetical fifth giant planet, reconstructing the outer solar system whilst preserving the orbits of the inner terrestrial bodies over long timescales (Batygin et al. 2012; Nesvorný & Morbidelli 2012). Such planet scattering events (Rasio & Ford 1996; Weidenschilling & Marzari 1996), applicable to any multi-body system, provide a potential explanation for the existence of the recently detected “free-floating” planets (e.g. Delorme et al. 2012; Liu et al. 2013; Luhman & Esplin 2014).

In addition to reconstructing the current orbital configuration of both large and small bodies in the solar system, models attempting to achieve a full description of the solar system’s early dynamical evolution must require the survival of the giant planets’ regular satellites

¹Dept. of Astronomy & Astrophysics University of Toronto, 50 St. George Street, Toronto, Ontario, Canada, M5S 3H4

²Centre for Planetary Sciences, University of Toronto, Department of Physical & Environmental Sciences, 1265 Military Trail, Toronto, Ontario, Canada, M1C 1A4

³Canadian Institute for Theoretical Astrophysics, 60 St. George Street, Toronto, Ontario, Canada, M5S 3H8

(e.g. [Deienno et al. 2014](#)). Regular satellites which are thought to form via accretion processes in circumplanetary disks ([Canup & Ward 2002](#); [Mosqueira & Estrada 2003](#)), are expected to form on prograde, low-eccentricity orbits that are nearly coplanar with the host’s equatorial plane and have relatively small semimajor axes. The current deviations of Callisto and Iapetus’ orbits from circular, uninclined orbits therefore limit how close an IG could have come to the gas giants in the early solar system.

In general, outer satellites, which are less tightly bound to the planet, will suffer larger perturbations during a close approach with an IG. In addition, the orbital eccentricities of these outer moons are only marginally damped through tides (which could otherwise mask the effects of early encounters). It is therefore the outermost regular satellites (Callisto around Jupiter and Iapetus around Saturn) which provide the most stringent constraints.

Specifically, [Deienno et al. \(2014\)](#) investigated whether the close encounters in the particular simulations of [Nesvorný & Morbidelli \(2012\)](#) (referred to as NM12), that best reproduced the giant planets orbital architecture, would excessively excite Callisto’s orbit. Given the interest in additional planets in the early solar system, we generalize this question to ask how likely it is to retain Callisto (Iapetus) at its observed orbit following an ejection of an IG by Jupiter (Saturn)? Although in the *jumping-Jupiter scenario* only Jupiter may be responsible for ejecting an IG, we include an analysis of close IG encounters with Saturn as we are more generally interested in early solar system instability models in which either gas giant could undergo close encounters with the solar system’s IGs. It also permits the direct comparison of the likelihood of retaining a Callisto-like satellite orbit to the likelihood of retaining an Iapetus-like satellite orbit following the ejection of an IG (see Sect. 6).

In Sect. 2 we discuss the relevant properties of the satellites of interest, Sect. 3 summarizes our methods of investigation, Sect. 4 & 5 present our study’s results, and Sect. 6 presents our calculation of the likelihood of reconciling satellite orbits following planetary encounters with present-day orbits. We conclude with a detailed discussion in Sect. 7 and a summary in Sect. 8.

2. SUMMARY OF SATELLITES: CALLISTO & IAPETUS

Callisto is the outermost Galilean satellite, moving on a nearly circular ($e = 0.007$) and uninclined ($i \sim 0.28^\circ$) orbit. Callisto’s orbital period is ~ 16.7 days and is the only Galilean satellite not locked in a mean-motion resonance ([Musotto et al. 2002](#)). Iapetus’ orbit is somewhat more eccentric ($e \sim 0.03$) and circles Saturn every ~ 79 days. Curiously, Iapetus exhibits a significantly inclined orbit possibly due to inclined planetary encounters between Saturn and an IG like those expected in the *jumping-Jupiter scenario* ([Nesvorný et al. 2014](#)). Current satellite orbital elements are summarized in Table 1. These data were obtained from JPL HORIZONS.⁴

While Callisto does not participate in a MMR like the other Galilean satellites, its eccentricity evolution is nevertheless secularly coupled to that of the inner moons ([Greenberg & Van Laerhoven 2011](#)). The eccentricities of the inner satellites are more easily damped

TABLE 1
SUMMARY OF GIANT PLANETS AND SATELLITES.

Planet	Jupiter	Saturn
$M_p (M_\odot)$	9.54×10^{-4}	2.86×10^{-4}
a_p (AU)	5.20	9.54
R_p (AU)	4.67×10^{-4}	3.89×10^{-4}
Satellite	Callisto	Iapetus
P_s (days)	16.69	79.33
$a_s (R_p)$	26.93	61.15
e_s	7.0×10^{-3}	2.83×10^{-2}
$i_s (^\circ)$	0.28	7.49

NOTE. — Data are from JPL HORIZONS: <http://ssd.jpl.nasa.gov/?horizons>

by tides than Callisto because of their smaller semimajor axes and as a result of the secular coupling, $e_{Callisto}$ is damped on timescales faster than expected for an isolated planet-satellite system that is tidally locked. We take this into account as described in Sect. 4.2 following numerical simulations of this effect by [Deienno et al. \(2014\)](#). Conversely, the eccentricity damping of Iapetus since the solar system’s instability phase, has been negligible ([Castillo-Rogez et al. 2007](#)).

3. METHODS

We model the evolution of an IG heading for a close approach with one of Jupiter or Saturn, and investigate the encounter’s effect on the gas giant’s satellites. We first determine viable encounter parameters that lead to the ejection of the IG. Within this set, we investigate if there are any satellites remaining around Jupiter (Saturn) with an orbit consistent with that of Callisto (Iapetus).

3.1. Numerical Model: Simulating Planetary Encounters

We consider a reduced-body subset of the solar system including the Sun, a satellite-hosting gas giant planet and an IG. The gas giant of mass M_p is initialized on a osculating, circular orbit with semimajor axis a_p . By approximating the gas giant’s orbit as circular, we remove any dependence on its orbital phase at the epoch of encounter; t_{enc} . Because the mass of the ejected IG is not well constrained, we select a fiducial value approximately equal to the mass of Uranus ($M_I = 5 \times 10^{-5} M_\odot$) as was used by NM12. A system of Keplerian satellites is placed in orbit around the gas giant (see Sect. 3.2 for a detailed description of satellite orbits).

To limit the number of encounter parameters and computational cost of our survey, we assume a coplanar geometry (we present a more detailed discussion of the effect of inclined encounters in Sect. 7.1). Thus, at closest approach the IG’s velocity is perpendicular to its separation vector from the gas giant and the encounter is fully specified at this time (t_{enc}) by the impact parameter b , the relative planet velocity v_{rel} , and the phase angle θ (see Fig. 1).

We linearly step the impact parameter outward from $b_{min} = 0.02$ AU until encounters no longer lead to ejections. [Deienno et al. \(2014\)](#) found that close encounters with $b < b_{min}$ excessively excite the Galilean satellites; our estimates in Sect. 6 for the likelihood of retaining the observed satellite orbits following an ejection therefore represent a conservative overestimate due to our comparatively gentle ejections. However, we note that values

⁴ <http://ssd.jpl.nasa.gov/?horizons>

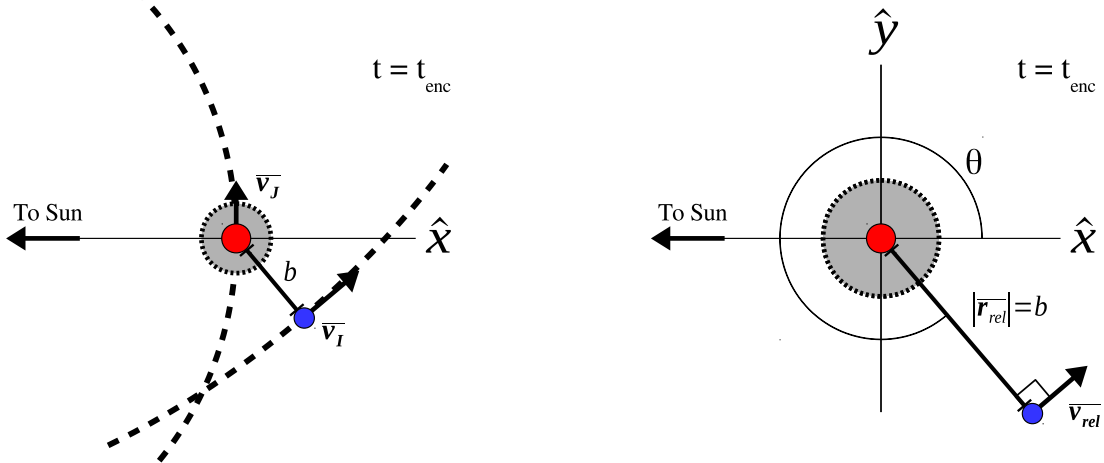


FIG. 1.— Pictorial representations of a close planetary encounter between a gas giant (*larger, red planet*) and an unspecified ice giant (IG; *smaller, blue planet*) at the epoch of encounter t_{enc} . The coplanarity of planetary encounters permits analysis solely in the xy -plane ($z = 0$). *Left*: the heliocentric reference frame with the Sun, at a distance of the gas giant’s semimajor axis, aligned with the \hat{x} axis. The planet’s instantaneous velocity vectors are shown along with their trajectories (*dashed lines*) in the vicinity of t_{enc} . *Right*: the reference frame is centered on the gas giant and is zoomed-in to depict the phase angle θ ; the angle between the \hat{x} axis and the IG’s position vector (\mathbf{r}_{rel}) at t_{enc} , measured in the counter-clockwise direction. Here, $\theta \approx 310^\circ$. At t_{enc} , the magnitude of the IG’s relative position vector is equal to the impact parameter b and is orthogonal to the relative velocity vector \mathbf{v}_{rel} . In both diagrams, the *dotted grey rings* represent the ring of regular satellites in orbit around the gas giant. The scale used here is approximate as these schematics are not intended to be exact, but instead, are included to aid in the reader’s visualization of the experimental setup.

smaller than b_{min} are less likely due to the reduced encounter cross-section at small radii. We estimate the size of this effect by including a reduced simulation sample with $b < b_{min}$ and find that our final results (Sect. 6) changed (fractionally) by $\lesssim 12\%$.

To determine which encounter parameters are capable of ejecting the IG, we uniformly sample 20,000 parameter combinations within $b \in [b_{min}, 0.1 \text{ AU}]$, $v_{rel} \in [1, 5]v_{esc}$, and $\theta \in [0, 2\pi)$, where $v_{esc} = \sqrt{2GM_p/b}$. We then remove any unphysical encounters in which the IG is unbound from the Sun prior to the encounter. In the cases of Jupiter and Saturn we find $N_{sim} = 278$ and $N_{sim} = 274$ valid parameter combinations respectively.

To simulate an encounter with the aforementioned parameters from Fig. 1, we integrate *backwards* in time until the absolute separation of the planets $|\mathbf{r}_I - \mathbf{r}_p| \geq 2 \text{ AU}$. At this separation a satellite with a Callisto-like or Iapetus like orbit feels a force from its host which is $> 10^4$ times greater than that felt from the IG. The positions and velocities of all three massive bodies are then used as initial conditions for the *forward* simulations which include the satellites. These simulations are integrated *forward* in time towards the encounter at $t = t_{enc}$ and are halted at $t = 2t_{enc}$. After $2t_{enc}$ the influence of the IG on the satellites is again negligible and satellite orbits are no longer perturbed by the IG’s influence. In order for close encounters with $b < 0.1 \text{ AU}$ to be possible, numerous ‘soft’ encounters between the gas giants and IG, prior to t_{enc} , were needed in order to build-up the IG’s eccentricity. These encounters will supply a small perturbation to regular satellite orbits that, on average, increase satellite eccentricity over time (see Nesvorný et al. (2014) Fig. 4). However, the effect of encounters on satellite orbits is strongly dependent on b , which is much larger than 0.1 AU for ‘soft’ encounters. We are there-

fore only concerned with the strongest (final) encounter which leads to ejection of the IG as its effect dominates the final satellite orbits.

Finally, we do not include the perturbations from the satellite host’s oblateness. This should be a good approximation since the encounter timescale with the IG is much shorter than the precession timescales of the satellites due to the non-spherical shape of its host planet.

3.2. Numerical Model: Initializing Satellites

In each encounter simulation, we include a ring of Callisto or Iapetus analog satellites around the gas giant planet. The satellite ring consists of $N = 100$ non-interacting test particles with azimuthal positions randomly sampled from a uniform distribution between 0 and 2π as to remove any azimuthal dependence at t_{enc} . Modelling the satellite system as an ensemble of test particles ensure that the orbital evolution of the satellites is governed solely by gravitational interactions with the host planet and perturbations from the IG and the Sun.

The semimajor axes of the satellites a_s are initialized to $\pm 1\%$ of the current orbital radius of Callisto or Iapetus. This fractional deviation is chosen to be on the order of the observed satellite eccentricities e_s (see Table 1). Because changes in a_s and e_s are related through changes in the satellites’ angular momentum, it is unlikely that larger shifts in a_s would be reconcilable with the observed e_s assuming that each satellite formed out of a circumplanetary disk on a circular orbit (Canup & Ward 2002; Mosqueira & Estrada 2003). Satellites are initialized on nearly coplanar and circular orbits ($i \leq 0.1^\circ$, $e \leq 10^{-5}$) as expected from circumplanetary formation scenarios. Satellite particles are not allocated physical sizes as we do not account for particle collisions in our simulations.

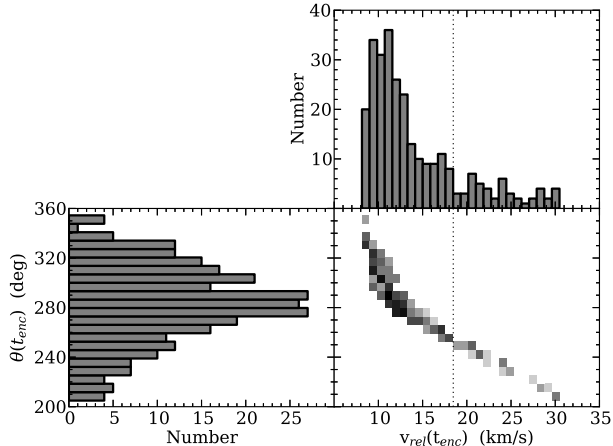


FIG. 2.— Distributions of the IG phase angle (θ ; *bottom-left*) and relative planet velocity (*top-right*) at t_{enc} for encounters between Jupiter and an unspecified IG that resulted in the ejection of the latter. Relative planet velocities are uniquely determined by the impact parameter b and the specified fraction of the escape speed from Jupiter. *Bottom-right*: 2D histogram exhibiting the correlation between phase angle and relative velocity. The darkness of each bin is indicative of the logarithmic number of successful ejections. The *vertical dotted line* is indicative of the escape velocity from the Sun at the semimajor axis of Jupiter.

3.3. Numerical Code

We performed our simulations using the REBOUND N-body numerical code (Rein & Liu 2012). We employ the IAS15 integrator (Integrator and Adaptive Step-size control, 15th order; Rein & Spiegel 2015) whose adaptive timestepping ensures optimal resolution of the short satellite orbital periods and rapid encounter timescales.⁵

4. RESULTS OF ICE GIANT EJECTIONS BY JUPITER

Here we focus on simulations in which Jupiter is the satellite-hosting gas giant planet that ejects the hypothetical fifth giant planet from the solar system.

4.1. Properties of Encounters

Fig. 2 summarizes the properties of the planetary encounters which result in the ejection of the IG planet. We find $N_{sim} = 278$ such encounters. The greatest impact parameter we find capable of ejecting the IG is ≈ 0.05 AU.

All successful ejections involve closest approach in the lower hemisphere of the xy -plane in Jupiter’s reference frame ($180^\circ < \theta(t_{enc}) < 360^\circ$; see Fig. 1). As familiar from spacecraft gravity assists, an IG trailing Jupiter at t_{enc} will receive a positive velocity kick via their interaction. At these phase angles, the relative velocity vector is rotated by the encounter such that the IG’s inertial speed accelerates. Depending on b and v_{rel} , the encounter can potentially boost the IG to escape velocity from the solar system. From simple vector diagrams, the maximum increase to the IG velocity can be shown to occur when $\theta(t_{enc}) = 270^\circ$. Fig. 2 highlights this as the distribution of $\theta(t_{enc})$ peaks at $\sim 270^\circ$ where the encounter geometry is most conducive to ejecting the IG.

Low v_{rel} trajectories lead more often to ejection since Jupiter can more effectively deflect the IG’s path. We

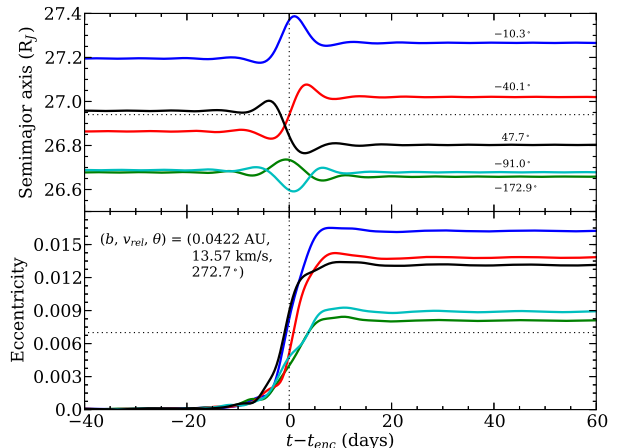


FIG. 3.— Evolution of five sample Jovian satellites as Jupiter undergoes a close encounter with an unspecified IG. The encounter parameters at t_{enc} : impact parameter b , relative planet velocity v_{rel} , and IG phase angle θ are shown in the legend of the lower panel. Each satellite’s azimuthal position relative to $\theta(t_{enc})$ is annotated in the upper panel. Vertical and horizontal *dotted lines* indicate the epoch of encounter and the current values of Callisto’s orbital elements respectively.

note that there are many encounters in which the velocity of the IG with respect to Jupiter at t_{enc} is greater than the escape speed from the solar system at Jupiter’s distance from the Sun. This is due to the IG being accelerated upon approach to the encounter which occurs deep in Jupiter’s gravitational well. Such cases consist of the IG becoming unbound from the solar system prior to the realization of the impact parameter at t_{enc} and are thus accelerated to super-escape speeds even before its closest approach to Jupiter.

The 2D histogram in Fig. 2 depicts the correlation between the relative velocity of the planets at the epoch of encounter and the phase angle in the jovian-centric reference frame. Encounters which occur with the IG at a smaller heliocentric distance than Jupiter ($\theta(t_{enc}) < 270^\circ$) require larger relative velocities in order to eject the IG. As the IG moves outwards (increasing θ) the relative velocities necessary to eject the IG decrease because the pull applied by Jupiter following the gravity assist is less efficient at decelerating the IG to sub-escape speeds given the IG’s trajectory.

4.2. Resulting Jovian Satellite Orbits

Close planetary encounters between Jupiter and the IG can result in significant perturbations to the orbits of the in-situ Jovian satellites. The time evolution of a_s and e_s for five sample Jovian satellites throughout one encounter simulation demonstrates this fact (Fig. 3).

The five sample satellites which are initialized on nearly circular orbits get kicked to moderately eccentric orbits by a planetary encounter with $b \approx 0.042$ AU and $v_{rel} \approx 13.57$ km/s. Hence, the characteristic encounter timescale is $b/v_{rel} \sim 5.3$ days or about one third of Callisto’s orbital period. The orbital perturbation therefore acts roughly as an impulse to the satellites making their azimuthal position at t_{enc} , a parameter of importance. Indeed, in Fig. 3 the satellites whose azimuthal positions are increasingly distant from $\theta(t_{enc})$ are on average less perturbed than satellites which are close to $\theta(t_{enc})$.

⁵ A short video from REBOUND depicting a close planetary encounter with a ring of regular satellites can be found [here](#).

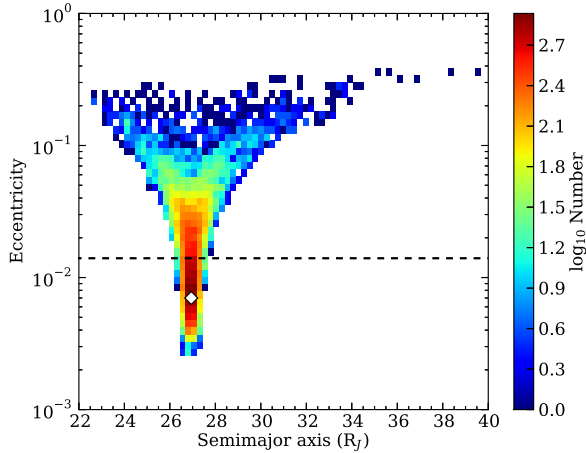


FIG. 4.— 2D histogram of the final average semimajor axes and eccentricities of Jovian satellites. The colorbar is indicative of the logarithmic number of satellites in each bin. The current values of Callisto’s semimajor axis and eccentricity are depicted on the plot as a *white diamond*. The *horizontal dashed line* highlights $2e_{Callisto}$ which marks the boundary between satellites that can ($e_s \leq 2e_{Callisto}$) and cannot ($e_s > 2e_{Callisto}$) be reconciled with Callisto’s current orbit.

In addition, the position of the satellite relative to $\theta(t_{enc})$ determines the direction of the satellite’s radial shift. For example, satellites immediately trailing the IG at t_{enc} will be pulled forward in their orbits (e.g. *red curve*) increasing a_s , whereas satellites immediately upstream of the IG at t_{enc} get pulled downward, thus decreasing a_s (e.g. *black curve*).

The average final orbital elements of all Jovian satellites are depicted in Fig. 4 and show close agreement with the results from Deienno et al. (2014) despite the broader investigation of the close encounter parameter space. Changes in a_s and e_s are coupled through the satellite’s orbital angular momentum. This effect is highlighted in Fig. 4, as satellites which are radially transferred to either a significantly larger or smaller semimajor axis are those which exhibit the largest deviation from a circular orbit.

For each satellite we define a reconcilable orbit to be when the satellite’s final average eccentricity is $\leq 2e_{Callisto}$ (recall $e_{Callisto} \approx 0.007$). The factor of 2 in our definition comes from the subsequent eccentricity evolution due to tidal damping of Callisto (Deienno et al. 2014, c.f. Fig. 7) and allows for Callisto to be excited beyond the present $e_{Callisto}$ at t_{enc} and consequently settle into its current orbital eccentricity in the 4 Gyrs following the solar system’s instability phase.

For the remainder of the paper we refer to the event of a simulated satellite’s final orbit being reconcilable with Callisto as *RS* for “reconcilable satellite”. The boundary dividing *RS* from non-*RS* satellites is depicted in Fig. 4 as a dashed horizontal line.

Final average e_s values are never ≥ 0.4 , implying that no Jovian satellite becomes unbound from Jupiter following the ejection of the IG. That is, the vast majority of planetary encounters that are capable of ejecting an IG from the solar system are not sufficiently violent to strip Jupiter’s regular satellites. This favours the possibility of Jupiter being able to eject an IG whilst retaining a regular satellite whose orbit is Callisto-like. We estimate

the likelihood in Sect. 6.

While the phase angle $\theta(t_{enc})$ is an important parameter in determining whether the IG is ejected, it has little effect on the fraction of perturbed satellites due to their uniformly distributed azimuthal positions around Jupiter. Therefore, for each b and v_{rel} we can marginalize over θ to show in Fig. 5 the fraction of satellites reconcilable with the orbit of Callisto after each encounter. Interpolating over the fraction of reconcilable Jovian satellites in (b, v_{rel}) space, the resulting high resolution contours at 10% and 50% are fitted with cubic functions and overplotted as solid and dashed curves respectively to aid in visualization of the different regions of the parameter space.

It is clear that as encounters become closer, the perturbation to e_s increases and the fraction of reconcilable satellites shrinks. Similarly, as the duration of encounters becomes longer (smaller v_{rel}), the timescale over which the perturbation is applied grows, thus increasing the deviation of satellite orbits from circular. Hence, forming and maintaining a Jovian satellite with a Callisto-like orbit favours encounters which are wide and fast.

We suggest that researchers simulating solar system formation scenarios can use Fig. 5 to estimate whether or not a given Jupiter/IG encounter is consistent with Jupiter’s current Galilean satellite orbits. We note that our requirement that the IG gets ejected only determines what regions of the plot are populated, hence the contours are useful guides regardless of whether or not the IG survives the encounter (and for any θ). We caution, however, that these will only be approximate due to our assumption of coplanarity. For a given b and v_{rel} , inclined encounters will increase the fraction of satellites whose eccentricities are reconcilable with current orbits. However, they will also tend to overly excite the satellite inclinations. We discuss this further in Sect. 7.1. For particular simulations that lie on the boundary of plausibility in Fig. 5, one could re-simulate the close approaches, including inclined encounters, following our setup to more accurately quantify the effect.

5. RESULTS OF ICE GIANT EJECTIONS BY SATURN

Here we focus on simulations in which Saturn is the satellite-hosting gas giant planet that ejects the hypothetical fifth giant planet from the solar system.

5.1. Properties of Encounters

The properties of planetary encounters between Saturn and an IG are summarized in Fig. 6. We find $N_{sim} = 274$ simulations which result in the IG being ejected by Saturn. The largest impact parameter that is still capable of ejecting the IG is nearly identical to the Jupiter/IG case; ≈ 0.05 AU. We perform an additional sampling of encounter parameters with $b > 0.05$ AU at an increased resolution to confirm that the largest impact parameter capable of ejecting the IG is nearly the same in both the Jupiter and Saturn cases rather than being a statistical anomaly due to the finite sampling of encounter parameters. We find that this limit is real and not an artifact of our sampling procedure. The physical interpretation of this similarity is beyond the scope of this paper.

Similar trends to those shown in Fig. 2 are observed. This should be expected because, modulo the variations in the physical parameters M_p and a_p , the Sat-

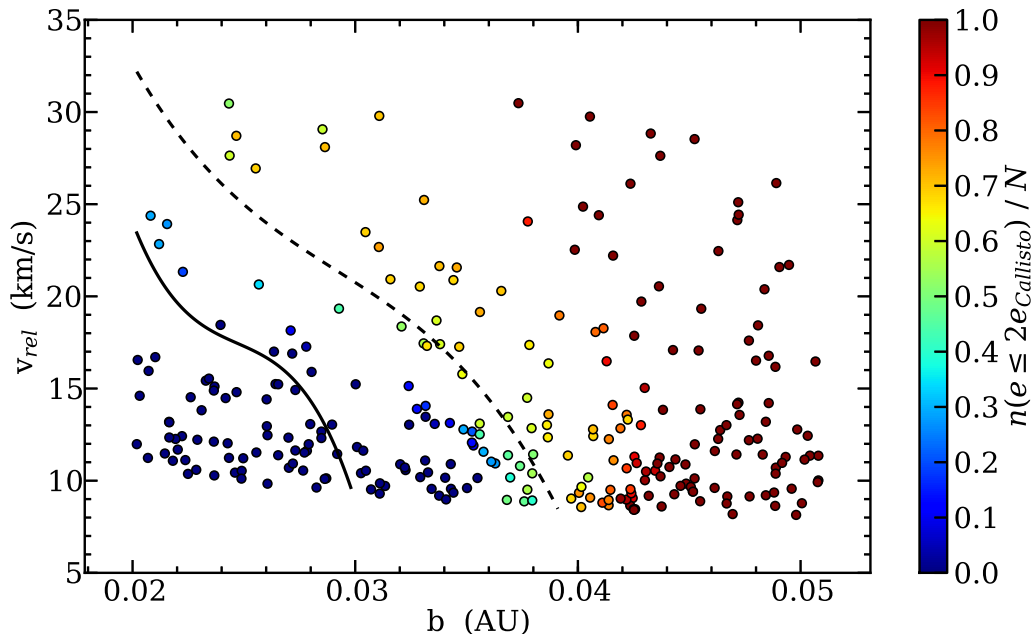


FIG. 5.— The fraction of reconcilable Jovian satellites as a function of the encounter’s impact parameter and relative planet velocity. The colorbar indicates the fraction of satellites whose final average eccentricity is less than or equal to $2e_{Callisto}$. Smoothed contours at 10% (solid line) and 50% (dashed line) assist in visualizing the different regions of the parameter space. The survival fractions shown here reveal that Jupiter has a reasonably large probability of ejecting an IG while retaining a Callisto-like satellite (see Sect. 6).

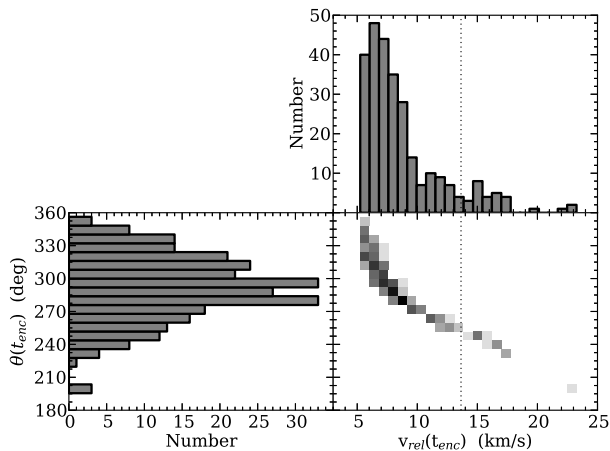


FIG. 6.— Same as Fig. 2 for encounters between Saturn and an unspecified IG. The vertical dotted line is indicative of the escape velocity from the Sun at the semimajor axis of Saturn.

urn/IG encounters investigated are fundamentally equivalent to those described in Sect. 4.1. With the exception of the decreased magnitude of v_{rel} by a factor of $\sqrt{M_{Sat}/M_{Jup}}$ on average, the set of successful scattered-by-Saturn simulations are statistically identical to those in the scattered-by-Jupiter simulations; i.e. the histograms in Figs. 2 and 6 exhibit the same behaviour.

5.2. Resulting Kronian Satellite Orbits

Similarly to the case of Jupiter ejecting the IG from the solar system, the Kronian satellite orbits will be perturbed as a result of the encounter between Saturn and the IG. As a result of the wide separation of Iapetus ($\sim 61 R_S$) and the similar nature of the encounters be-

tween an IG and either Jupiter or Saturn (Figs. 2 & 6), it is expected that such orbital perturbations will be more destructive to simulated satellite orbits than to those previously explored in Sect. 4. This notion is supported in Figs. 7, 8, and 9 when compared to their counterparts in the Jupiter/IG case (Figs. 3, 4, and 5) as the fraction of reconcilable Kronian satellites is systematically lower than in the Jupiter case.

The time evolution of a_s and e_s for five example satellites during a sample planetary encounter is shown in Fig. 7. This example is a particularly violent encounter with $b \approx 0.033$ AU and $v_{rel} \approx 5.87$ km/s as no satellite in this simulation has a resulting orbit that is reconcilable with Iapetus. One satellite, whose azimuthal position is only 4.6° from $\theta(t_{enc})$, is ejected from Saturn by the encounter. The encounter timescale ($b/v_{rel} \sim 9.6$ days) is much less than the orbital period of Iapetus making the effect of the encounter behave approximately as an impulse.

The average final orbital elements of all Kronian satellites after each unique encounter are depicted in Fig. 8. The black contours in Fig. 8 are representative of the final orbital elements of the Jovian satellites from Fig. 4 to aid in visual comparison between the final orbits of Jovian satellites to Kronian satellites following similar close planetary encounters. This shows that the wide-separation of the simulated Kronian satellites makes them more susceptible to excessive orbital perturbations.

The event RS in the Saturn/IG case is defined similarly to the Jupiter/IG case and is achieved by Kronian satellites whose final average $e_s \leq e_{Iapetus}$. As noted earlier, the eccentricity evolution of Iapetus since the solar system’s instability phase is negligible (Castillo-Rogez et al. 2007) thus we assume that resulting orbits from our sim-

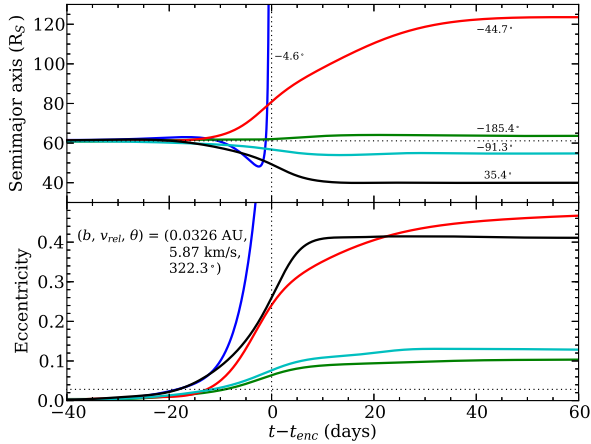


FIG. 7.— Same as Fig. 3 featuring the evolution of five sample Kronian satellites as Saturn undergoes a close encounter with an unspecified IG. Vertical and horizontal dotted lines indicate the epoch of encounter and the current values of Iapetus’ orbital elements respectively.

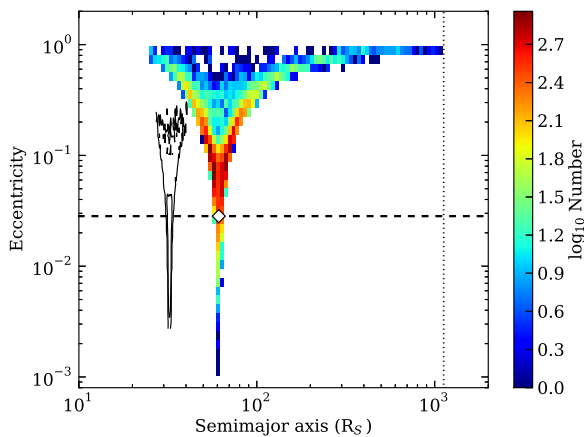


FIG. 8.— Similar to Fig. 4 for the Kronian satellites with the inclusion of Saturn’s Hill radius ($\sim 1100 R_S$; vertical dotted line) and contours of the 2D histogram shown for Jupiter (Fig. 4) for direct comparison. The horizontal dashed line highlights $e_{Iapetus}$ which marks the boundary between satellites that can ($e_s \leq e_{Iapetus}$) and cannot ($e_s > e_{Iapetus}$) be reconciled with Iapetus’ current orbit. Note the logarithmic x-axis.

ulations will go largely unchanged to the present day. The boundary dividing RS from non- RS is depicted in Fig. 8 as a dashed horizontal line.

As noted in Sect. 4.2, no Jovian satellite becomes more eccentric than 0.4 whereas a sizable fraction of Kronian satellites become equivalently or excessively excited including a subset of Kronian satellites whose final average e_s is approximately unity. Furthermore, we find that $\sim 6\%$ of sampled Kronian satellites are sufficiently excited to final $e_s > 1$. The orbital elements of these ejected satellites are not included in Fig. 8. It is clear that the perturbations to the Kronian satellites resulting from close encounters, are on average much stronger and capable of stripping Iapetus-like satellites from the Kronian system. The large fraction of satellites perturbed beyond the orbit of Iapetus makes it statistically diffi-

cult for Saturn to have ejected an IG whilst retaining an Iapetus-like regular satellite. We formally estimate the likelihood of reconciling Iapetus’ orbit in Sect. 6.

The effect of encounter properties on the resulting Kronian satellite orbits is shown in Fig. 9. For each encounter with a given impact parameter and relative planet velocity, the fraction of Kronian satellites whose final orbit is reconcilable with the current orbit of Iapetus is shown. Approximate contours of 10% and 50% fractions are over-plotted. The 10% contour is computed identically to the contours in Fig. 5 (i.e. cubic interpolation). However, the 50% contour lacks a sufficient number of points to perform a robust cubic interpolation. Therefore we opt for a linear fit in its place. It is clear that the region of the (b, v_{rel}) parameter space in which $\geq 50\%$ of the Kronian satellites are reconcilable with Iapetus’ orbit is very small compared to the Jovian satellites with only five unique ejections sampled there.

The effects of b and v_{rel} on resulting satellite orbits are nearly identical to those shown in Fig. 5. One interesting difference which is unique to Saturn/IG encounters is that regardless of how close the encounter is, if the encounter is sufficiently long ($v_{rel} \lesssim 8$ km/s), then $< 10\%$ of satellites will be reconcilable with Iapetus. This is in contrast to the Jovian satellite case where even the slowest encounters could retain a high fraction of Callisto-like satellites if the encounter’s impact parameter is large. Another important feature to note is that no Saturn/IG encounter resulting in the ejection of the latter is guaranteed to preserve an Iapetus-like satellite. That is, even the least violent encounters leading to ejection are only capable of preserving a maximum of $\sim 70\%$ of the in-situ Iapetus-like satellites.

Fig. 9 contains information on the likelihood that Iapetus survives an IG ejection by Saturn with a particular $b(t_{enc})$ and $v_{rel}(t_{enc})$ when the mutual inclination of the encounter is near zero. Similarly to the Jupiter/IG encounter case, we suggest that researchers simulating solar system formation scenarios can use Fig. 9 to estimate whether or not a given Saturn/IG encounter is consistent with Iapetus’ current orbit in the limit of un-inclined planetary encounters.

6. LIKELIHOOD OF RECONCILING SATELLITE ORBITS FOLLOWING ICE GIANT EJECTIONS

6.1. Methodology

The resemblance of the final average orbits of the Jovian and Kronian satellites (Figs. 4 and 8) to the current orbits of Callisto and Iapetus can, in principle, be used to compute the likelihood of a fifth giant planet getting ejected by either of the gas giant planets in the early solar system. If such an event were to have occurred, it must be consistent with the satellite orbits presently observed. The likelihood of an IG getting ejected by either gas giant requires the likelihood of the current orbits of Callisto or Iapetus being reconciled by simulated satellites after an IG ejection. A successful event in which the resulting orbit of a simulated Jovian (Kronian) satellite is reconcilable with Callisto’s (Iapetus’) current orbit is referred to as RS for “reconcilable satellite”.

Given that an IG gets ejected in all simulations (event IGE ; “ice giant ejected”), for the i^{th} satellite in the j^{th} simulation, we record whether or not the event RS is achieved by

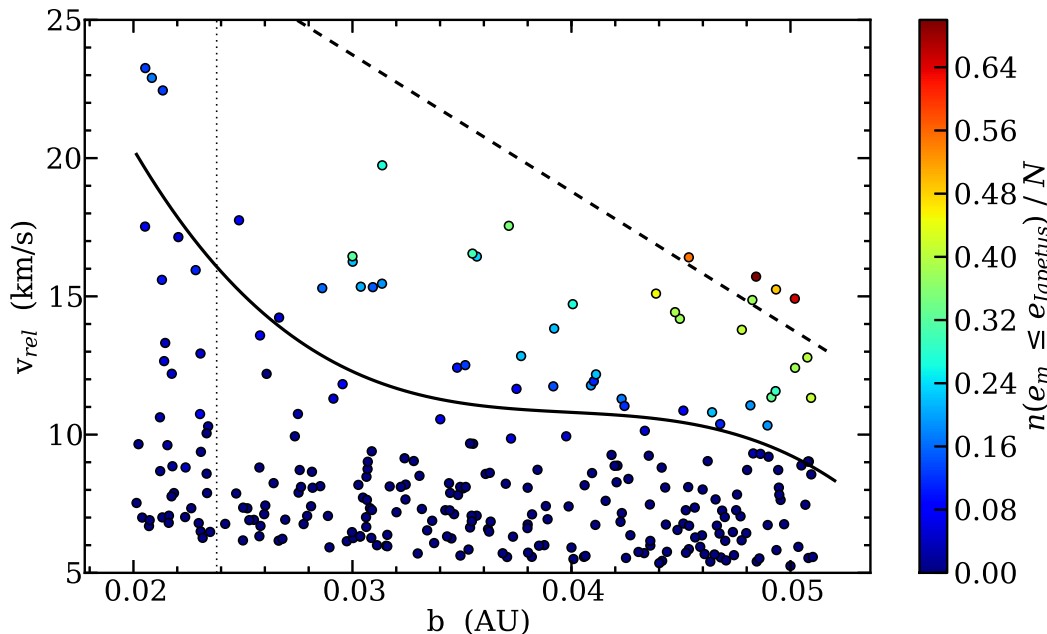


FIG. 9.— Same as Fig. 5 for the Kronian satellites. The colorbar indicates the fraction of satellites whose final average e_s is less than or equal to $e_{Iapetus}$. The vertical dotted line indicates Iapetus’s current semimajor axis. The survival fractions here reveal that Saturn has a small probability of ejecting an IG while retaining an Iapetus-like satellite if we assume that Iapetus formed like a regular satellite out of a circumplanetary disk.

$$p_{i,j}(RS|IGE) = \begin{cases} 1 & \text{if } RS \\ 0 & \text{if not } RS. \end{cases} \quad (1)$$

However, not all planet orbits in our ejection simulations are statistically relevant. Our adopted methodology for determining which encounter parameters result in an ejection is heavily biased towards initially high-eccentricity orbits of the IG ($e_I \gtrsim 1$) which are not long-term stable and therefore are uncommon in nature. This bias naturally arises because it is easier to kick the IG to $e_I > 1$ if e_I is initially very close to unity. Therefore in each simulation j , each satellite’s likelihood of RS must be weighted by the likelihood of the IG having an initially bound orbit with $e_{I,j}$, where $e_{I,j}$ is the IG’s initial eccentricity in the j^{th} simulation.

The corresponding weighting function $W(e_{I,j})$ is modelled by the distribution of planet eccentricities observed in a statistically significant number of exoplanetary systems as the eccentricity distribution of solar system bodies is insufficient as it can only be derived in the limit of small number statistics. These data are recovered from the www.exoplanets.org database (Han et al. 2014) and only include RV exoplanet detections with Doppler variation semi-amplitude $K/\sigma_K > 5$ (neglect low signal-to-noise observations). We find that our results do not sensitively depend on whether we focus on RV detections or the full catalogue of exoplanets with orbital solutions. The distribution of planet eccentricities is shown in Fig. 10. Due to variations in empirically derived eccentricity distributions we consider three proposed analytical forms of the distribution. Namely a Beta probability density function (PDF) (Kipping 2013), a Rayleigh PDF plus decaying exponential (Juric & Tremaine 2008; Steffen et al. 2010), and the model from Shen & Turner

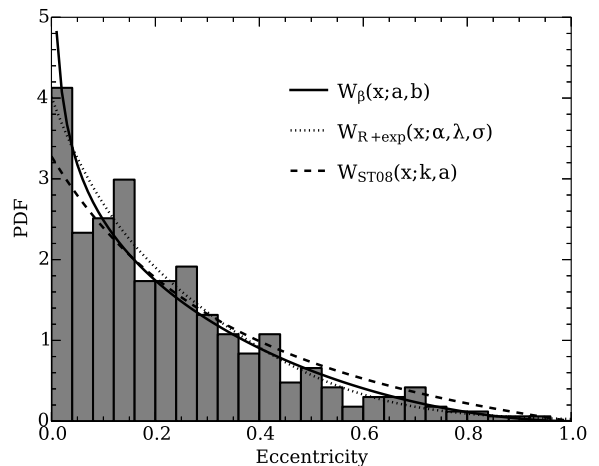


FIG. 10.— Histogram of the planet eccentricities used to model the weighting function $W(e_{I,k})$ in Eqs. 2 and 3. The three analytical models used to fit the distribution are overplotted (solid line: Beta PDF, dotted line: Rayleigh PDF plus exponential, dashed line: model from Shen & Turner (2008); see text).

(2008). We use a Levenberg-Marquardt least squares algorithm to fit for each PDF’s unique parameters. A summary of the adopted distributions including fitted parameters is given in Table 2 and each fitted weighting function is over-plotted in Fig. 10. Differences in $W(e_{I,j})$ from adopting three unique PDFs results in $\sim 6\%$ variance among computed likelihoods.

While we take the known exoplanet orbital eccentricities as our nominal distribution, this sample is obviously biased by the requirement that systems be stable. If early on, the solar systems ice giants moved on significantly more elliptical paths than the known exoplanets, it

TABLE 2
ANALYTICAL FITS TO THE PLANET ECCENTRICITY DISTRIBUTION.

PDF Name	PDF	Parameter 1	Parameter 2	Parameter 3
Beta	$W_\beta(x; a, b) = \frac{1}{B(a, b)} x^{a-1} (1-x)^{b-1}$	0.786 ± 0.055	2.764 ± 0.167	-
Rayleigh + exponential	$W_{R+\exp}(x; \alpha, \lambda, \sigma) = \frac{x(1-\alpha)}{\sigma^2} \exp\left(-\frac{x^2}{2\sigma^2}\right) + \alpha\lambda \exp(-\lambda x)$	0.782 ± 0.301	5.131 ± 2.342	0.266 ± 0.061
ST08	$W_{ST08}(x; k, a) = \frac{1}{k} \left(\frac{1}{(1+x)^a} - \frac{x}{2^a} \right)$	0.305 ± 0.012	3.413 ± 0.309	-

NOTE. — Parameter columns are written in the order in which they appear in the functional form $W(x; \dots)$, shown in the PDF column. We write the independent variable of planet eccentricity as x to make the distinction between eccentricity and Euler’s number $e \approx 2.7182818$.

would be easier to eject planets while keeping Jupiter and Saturn’s satellites on nearly circular orbits, raising the likelihood of reconciling satellite orbits. However, this scenario would require a substantial amount of damping to subsequently recircularize the surviving planets orbits, and if eccentricities reached such high values, one might expect to also lose Uranus and Neptune. These considerations may be interesting directions for future work.

One must additionally weight $p_{i,j}$ by the simulation’s impact parameter b_j , since wider encounters should occur more frequently. Given our coplanar setup, the differential interaction cross-section for a given impact parameter scales linearly with b_j rather than with b_j^2 as is true in the full 3D case. We find that our results do not sensitively depend on this distinction. We therefore assume $W'(b_j) \propto b_j$.

The distribution of $e_{I,j}$ is not explicitly prescribed and is instead determined from the encounter parameters (b, v_{rel}, θ) . The resulting distribution of $e_{I,j}$ is not sampled uniformly, unlike the distribution in b or θ , implying that the step size Δe_I when integrating over IG eccentricities is not constant throughout the domain. Hence, simulations sample IG eccentricity bins of various widths which are taken into account when computing the likelihood function by calculating the width of IG eccentricity bins among the N_{sim} simulations. In this way, the subspace of IG eccentricities which is over-sampled gets averaged over. Similar factors Δb_j and $\Delta \theta_j$ are included but are constants, because the parameters are sampled uniformly, and therefore do not affect the resulting likelihood.

Combining the aforementioned effects into the likelihood of obtaining a reconcilable satellite (*RS*) orbit given an IG ejection (*IGE*), we write

$$P(RS|IGE) = \frac{1}{\mu} \sum_{i=1}^N \sum_{j=1}^{N_{sim}} p_{i,j}(RS|IGE) W(e_{I,j}) W'(b_j) \Delta e_{I,j} \Delta b_j \Delta \theta_j \quad (2)$$

where

$$\mu = N \sum_{j=1}^{N_{sim}} W(e_{I,j}) W'(b_j) \Delta e_{I,j} \Delta b_j \Delta \theta_j, \quad (3)$$

is the normalization factor of the weighted mean and we are careful to account for the fact that our uniform sampling of (b, v_{rel}, θ) leads to a non-uniform distribution of $e_{I,j}$.

6.2. Likelihoods

From our $N_{sim} = 278$ ejection simulations by Jupiter, each with N satellites, we calculate that the likelihood of Jovian satellite orbits remaining consistent with the observed orbit of Callisto, is $\sim 42\%$. This value is the median of the results we obtained from adopting the three distinct eccentricity weighting functions discussed in Sect. 6.1 (see Table 2). The median absolute deviation among the likelihoods is small; $\lesssim 1\%$.

By contrast, in our $N_{sim} = 274$ ejection simulations by Saturn, the likelihood of Kronian satellite orbits remaining consistent with Iapetus’ observed orbit is $\sim 1\%$, more than an order of magnitude less likely than for Callisto around Jupiter. The main reason for this wide likelihood disparity is that a given encounter will perturb Iapetus more strongly than Callisto because the former is less tightly bound to Saturn than the latter is to Jupiter. In this case, the median absolute deviation among the three eccentricity weighting functions is $\lesssim 0.6\%$ which is comparable to the likelihood itself.

7. DISCUSSION

To recapitulate, the above likelihoods assumed an IG ejection in a coplanar geometry, considering whether an initially circular Callisto (Iapetus) would have its orbital eccentricity excited beyond values reconcilable with its current orbit. We now consider these assumptions in turn, in order to interpret the results from our study and discuss possible implications of our work.

7.1. Effect of Inclined Encounters

To limit the computational cost of our study, we have restricted our analysis to planetary encounters with no mutual inclination. However, if planetary eccentricities are excited enough to permit orbit-crossing and ejections, one might expect comparably large orbital inclinations. During an inclined encounter, some of the applied torque goes into realigning Callisto’s (Iapetus’) orbital plane so that, on average, the perturbations to a_s and e_s are reduced as some energy goes into increasing i_s .

A preliminary analysis of inclined encounters with mutual inclination $i(t_{enc}) = 5^\circ$ effectively revealed no change to the final satellite orbital elements compared to uninclined, but otherwise equivalent, encounters. In a more heavily inclined test case with $i(t_{enc}) = 45^\circ$, we found that, on average, the final e_s were *smaller* by $\gtrsim 0.01$ than in the uninclined case.

Therefore, by limiting our investigation to coplanar encounters, we are sampling the largest possible perturbations to e_s without affecting i_s . The introduction of inclined encounters would thus raise the likelihoods quoted in Sect. 6.2. However, such a 3D case would additionally excite the satellite inclinations. As mentioned by [Deianno et al. \(2014\)](#), these inclinations may provide more rigorous constraints on planetary encounters be-

cause even in cases where eccentricity damping is important, the tidal evolution of the inclinations is effectively null. A generalization of this study would therefore consider the combined constraint from the satellites’ orbital eccentricities and inclinations. However, the uncertainties in the likelihoods we compute in Sect. 6.2 are dominated by the large uncertainties in the planetary orbital eccentricities (and inclinations) early in the solar system. We therefore believe that our simplified analysis considering only the orbital eccentricities captures the correct likelihoods at the approximate level allowable by our current state of knowledge.

As a rough check, in a fully 3D case, the differential cross-section for encounters of a given impact parameter would scale as b_j^2 rather than as b_j . Using the full data set from our coplanar simulations, but adopting this new scaling for $W'(b_j)$ in Eqs. 2 and 3, we find that our results do not change discernibly. Specifically, in the Jupiter case our results change from $\sim 42\%$ to 54% and from $\sim 1.1\%$ to 1.3% in the Saturn case. This is certainly within the errors of our uncertain knowledge of the planetary orbits’ initial eccentricities and inclinations and therefore does not appreciably change the interpretation of our results.

7.2. Interpretation of Results

We conclude that Jupiter could plausibly have ejected an IG from the solar system. Nearly half of the hypothetical set of ejections that were modelled in Sect. 6.2 keep Callisto on an orbit which is reconcilable with the one we observe today. Put another way, we conclude that Callisto’s orbit cannot meaningfully constrain whether or not Jupiter ejected an additional IG in the early Solar System. Nevertheless, this is an important test for the fifth-giant-planet hypothesis to pass, thus providing more stringent evidence for its plausibility.

Interpretation of our results in the Saturn case is more subtle. We showed in Sect. 6.2 that an initially circular Iapetus orbit gets overly excited by a single ejection event $\sim 99\%$ of the time. This suggests that Saturn is not capable of ejecting an IG mass planet from the solar system.

But did Iapetus originally move on a circular path, as expected if it formed out of a circumplanetary disk? Starting with a circular orbit, all encounters act to raise the eccentricity. But if the moon’s initial path were instead elliptical, some ejection geometries could act to lower the eccentricity, complicating the constraint that we nominally set. Perhaps one reason to doubt that Iapetus formed from a circum-kronian disk is that it is substantially inclined ($\approx 8^\circ$) to the local equilibrium plane that one would expect it to follow.

So what caused this aberrant inclination? Hamilton (2013) recently suggested that Iapetus could indeed have formed on a circular orbit from a disk in its equilibrium plane, and subsequent collisions between Saturn’s inner moons could have instead tilted the equilibrium plane for the exterior moons by the requisite amount. In this case, our study implies that Saturn likely did not eject an IG from the solar system because Iapetus’ relatively low eccentricity orbit cannot be reconciled with IG ejections by Saturn. On the other hand, Iapetus’ inclination could be the signature of an ejection event itself. Nesvorný et al. (2014) recently studied such a scenario trying to simulta-

neously match Iapetus’ current orbital eccentricity and inclination using simulations of the specific early solar system dynamical instabilities from NM12. They show that some cases are capable of sufficiently exciting Iapetus’ orbital inclination whilst maintaining a low orbital eccentricity even for encounters as close as those considered in this study but not necessarily leading to ejection of the IG.

In the Kronian case, therefore, the interpretation depends critically on the formation mechanism for Iapetus, which is currently unknown. If Iapetus’ inclination is the result of collisions between inner moons (Hamilton 2013), our results show that Saturn is unlikely to have ejected an IG from the early Solar System. By contrast, if Iapetus’ orbit is fully explainable through close planetary encounters, Nesvorný et al. (2014) showed that this requires many such close approaches which might be capable of ejecting the IG.

7.2.1. Single-Encounter Assumption

We argue that the sole consideration of the final gas giant/IG encounter leading to ejection of the latter, is a sufficient measure of how close planetary encounters will modify regular satellite orbits. Nesvorný et al. (2014) showed for Iapetus, which is more susceptible to dynamical perturbations than Callisto, that numerous ‘soft’ encounters prior to ejection have a fractional effect on satellite eccentricity compared to the eccentricity kick typically felt during the final encounter (Fig. 4 and 8). It should be noted that inclusion of numerous ‘soft’ encounters prior to ejection would be detrimental to the computed likelihoods $P(RS|IGE)$ thus emphasizing that our results represent a conservative, best-case scenario.

7.2.2. Close Encounters Without Ejection

Due to the phase angle of an encounter being random, it is possible for a close encounter to have occurred at $0^\circ < \theta < 180^\circ$ and is subsequently not included in our likelihood calculation as all ejection events occurred at $180^\circ \leq \theta \leq 360^\circ$ (see Figs. 2 and 6). Any close encounter that does not lead to an ejection would still perturb regular satellite orbits, making their orbits prior to an IG ejection event, non-circular. The effect of an increased initial eccentricity reduces $P(RS|IGE)$, again making our calculation a conservative upper limit. However, because the frequency of close encounters with $0^\circ < \theta < 180^\circ$ is equivalent to the frequency of close encounters with $180^\circ \leq \theta \leq 360^\circ$, the effect on $P(RS|IGE)$ of close encounters without an ejection will only differ from our calculated values by a factor of order unity, such that we capture the correct order of magnitude on $P(RS|IGE)$.

7.3. Additional Considerations

One sought after quantity relating to this work is the probability of an IG getting ejected by either gas giant given that the orbit of Callisto or Iapetus can be reconciled; $P(IGE|RS)$. Using Bayes’ theorem, this quantity could in principle be computed with knowledge of the likelihood functions calculated in this paper but also requires the independent probability of the IG getting ejected ($P(IGE)$; see NM12) and the normalization factor by the probability of a satellite exhibiting the current

orbit of one of the wide-separation satellites ($P(RS)$). Despite the abundance of work done on the latter (e.g. Canup & Ward 2002; Estrada & Mosqueira 2006; Ward & Canup 2010; Crida & Charnoz 2012; Hamilton 2013; Heller et al. 2015), precise constraints on $P(RS)$ are difficult to compute.

Also, a robust calculation of the likelihood of ejecting an IG from the solar system would require the event to be consistent with a vast number of constraints imposed by solar system bodies of which the orbital constraint RS imposed by Callisto or Iapetus is just one. Therefore, such a calculation is not practical. However, consistency checks of IG ejections by a gas giant, such as those presented in this study, help to substantiate the proposed existence of a fifth giant planet. *Based on our current understanding, which includes the main results of our study, there is little evidence demonstrating that an additional IG mass planet could not have existed in the early solar system.*

8. SUMMARY

Several studies trying to match the solar system’s current orbital architecture argue for an early period of frequent planetary encounters (e.g. Tsiganis et al. 2005; Brasser et al. 2009; Morbidelli et al. 2009; Levison et al. 2011). In addition, Nesvorný (2011) found that adding a fifth giant planet to the solar system, which is subsequently ejected, better matches the current orbits of the remaining giant planets. In this paper, we therefore study whether such an ejection by either Jupiter or Saturn is reconcilable with the current observed orbits of their outermost regular satellites, Callisto and Iapetus. Our main conclusions are as follows:

- The properties of planetary encounters (i.e. impact parameter, relative planet velocity, and encounter

geometry) between Jupiter or Saturn and an unspecified ice giant, which are sufficiently violent to eject the latter, exhibit similar trends.

- The current (dynamically cold) orbit of the widest-separation Galilean satellite Callisto, has a significant likelihood ($\sim 42\%$) of being reconciled following the ejection of an ice giant planet from the solar system by Jupiter.
- Given the observed difficulty in reconciling the orbit of Iapetus with simulated Kronian satellites following an ejection event, the likelihood of Saturn ejecting an ice giant from the solar system is determined to be unlikely; likelihood $\sim 1\%$.
- However, we note the caveat that this interpretation is heavily dependent on the assumed formation scenario of Iapetus out of circum-kronian disk. Currently, the formation of Iapetus is largely uncertain.

We caution that these likelihoods should not be interpreted in an absolute sense. Rather, they are useful in showing that it is much easier for Jupiter to have ejected an ice giant than it is for Saturn. The evident plausibility of Jupiter being able to eject an IG thus supports the hypothesis of a fifth giant planet’s existence in the early solar system.

RC would like to thank H. Rein, M. Van Kerkwijk, and R. Gomes for useful discussions and suggested improvements to the manuscript. RC also thanks D. Nesvorný for numerical test cases of the solar system instabilities from NM12. Simulations in this paper made use of the collisional N-body code REBOUND which can be downloaded freely at <http://github.com/hannorein/rebound>. This research has made use of the Exoplanet Orbit Database and the Exoplanet Data Explorer at exoplanets.org.

REFERENCES

Batygin, K., Brown, M. E., & Betts, H. 2012, ApJ, 744, L3
 Brasser, R., Morbidelli, A., Gomes, R., Tsiganis, K., & Levison, H. F. 2009, A&A, 507, 1053
 Canup, R. M., & Ward, W. R. 2002, AJ, 124, 3404
 Castillo-Rogez, J. C., Matson, D. L., Sotin, C., et al. 2007, Icarus, 190, 179
 Crida, A., & Charnoz, S. 2012, Science, 338, 1196
 Deienno, R., Nesvorný, D., Vokrouhlický, D., & Yokoyama, T. 2014, AJ, 148, 25
 Delorme, P., Gagné, J., Malo, L., et al. 2012, A&A, 548, A26
 Estrada, P. R., & Mosqueira, I. 2006, Icarus, 181, 486
 Fernandez, J. A., & Ip, W.-H. 1984, Icarus, 58, 109
 Gomes, R., Levison, H. F., Tsiganis, K., & Morbidelli, A. 2005, Nature, 435, 466
 Greenberg, R., & Van Laerhoven, C. 2011, ApJ, 733, 8
 Hahn, J. M., & Malhotra, R. 1999, AJ, 117, 3041
 Hamilton, D. P. 2013, in AAS/Division for Planetary Sciences Meeting Abstracts, Vol. 45, AAS/Division for Planetary Sciences Meeting Abstracts, 302.01
 Han, E., Wang, S. X., Wright, J. T., et al. 2014, PASP, 126, 827
 Heller, R., Marleau, G.-D., & Egon Pudritz, R. 2015, ArXiv e-prints, arXiv:1506.01024
 Jurić, M., & Tremaine, S. 2008, ApJ, 686, 603
 Kipping, D. M. 2013, MNRAS, 434, L51
 Levison, H. F., Bottke, W. F., Gounelle, M., et al. 2009, Nature, 460, 364
 Levison, H. F., Morbidelli, A., Tsiganis, K., Nesvorný, D., & Gomes, R. 2011, AJ, 142, 152
 Levison, H. F., Morbidelli, A., Van Laerhoven, C., Gomes, R., & Tsiganis, K. 2008, Icarus, 196, 258
 Liu, M. C., Magnier, E. A., Deacon, N. R., et al. 2013, ApJ, 777, L20
 Luhman, K. L., & Esplin, T. L. 2014, ApJ, 796, 6
 Malhotra, R. 1995, AJ, 110, 420
 Morbidelli, A., Brasser, R., Gomes, R., Levison, H. F., & Tsiganis, K. 2010, AJ, 140, 1391
 Morbidelli, A., Brasser, R., Tsiganis, K., Gomes, R., & Levison, H. F. 2009, A&A, 507, 1041
 Morbidelli, A., Levison, H. F., Tsiganis, K., & Gomes, R. 2005, Nature, 435, 462
 Morbidelli, A., Tsiganis, K., Crida, A., Levison, H. F., & Gomes, R. 2007, AJ, 134, 1790
 Mosqueira, I., & Estrada, P. R. 2003, Icarus, 163, 198
 Musotto, S., Varadi, F., Moore, W., & Schubert, G. 2002, Icarus, 159, 500
 Nesvorný, D. 2011, ApJ, 742, L22
 Nesvorný, D., & Morbidelli, A. 2012, AJ, 144, 117
 Nesvorný, D., Vokrouhlický, D., Deienno, R., & Walsh, K. J. 2014, AJ, 148, 52
 Nesvorný, D., Vokrouhlický, D., & Morbidelli, A. 2007, AJ, 133, 1962
 Rasio, F. A., & Ford, E. B. 1996, Science, 274, 954
 Rein, H., & Liu, S.-F. 2012, A&A, 537, A128
 Rein, H., & Spiegel, D. S. 2015, MNRAS, 446, 1424
 Shen, Y., & Turner, E. L. 2008, ApJ, 685, 553
 Steffen, J. H., Batalha, N. M., Borucki, W. J., et al. 2010, ApJ, 725, 1226
 Tsiganis, K., Gomes, R., Morbidelli, A., & Levison, H. F. 2005, Nature, 435, 459
 Ward, W. R., & Canup, R. M. 2010, AJ, 140, 1168

Weidenschilling, S. J., & Marzari, F. 1996, *Nature*, 384, 619